Electronic Supplementary Information

Assessment of the UCST-type liquid-liquid phase separation mechanism of imidazolium-based ionic liquid, [C_8mim][TFSI], and 1,4-dioxane by SANS, NMR, IR, and MD simulations

Masahiro Kawano[a], Koichiro Sadakane[b], Hiroki Iwase[c], Masaru Matsugami[d], Bogdan A. Marekha[e], Abdenacer Idrissi[f], and Toshiyuki Takamuku[g,*]

[a] *Department of Chemistry and Applied Chemistry, Graduate School of Science and Engineering, Saga University, Honjo-machi, Saga 840-8502, Japan*

[b] *Faculty of Life and Medical Sciences, Doshisha University, 1-3 Tatara Miyakodani, Kyotanabe, Kyoto 610-0394, Japan*

[c] *Comprehensive Research Organization for Science and Society (CROSS), 162-1 Shirakata, Tokai, Ibaraki 319-1106, Japan*

[d] *Faculty of Liberal Arts, National Institute of Technology (KOSEN), Kumamoto College, 2659-2 Suya, Koshi, Kumatomo 861-1102, Japan*

[e] *Department of Biomolecular Mechanisms, Max Planck Institute for Medical Research, 29 Jahnstr., 69230 Heidelberg, Germany*

[f] *University of Lille, CNRS, UMR 8516 -LASIRe- Laboratoire Avancé de Spectroscopie pour les Interactions la Réactivité et l'environnement, F-5900 Lille, France*

[g] *Department of Chemistry and Applied Chemistry, Faculty of Science and Engineering, Saga University, Honjo-machi, Saga 840-8502, Japan*

*Corresponding Author
Toshiyuki Takamuku
E-mail: takamut@cc.saga-u.ac.jp

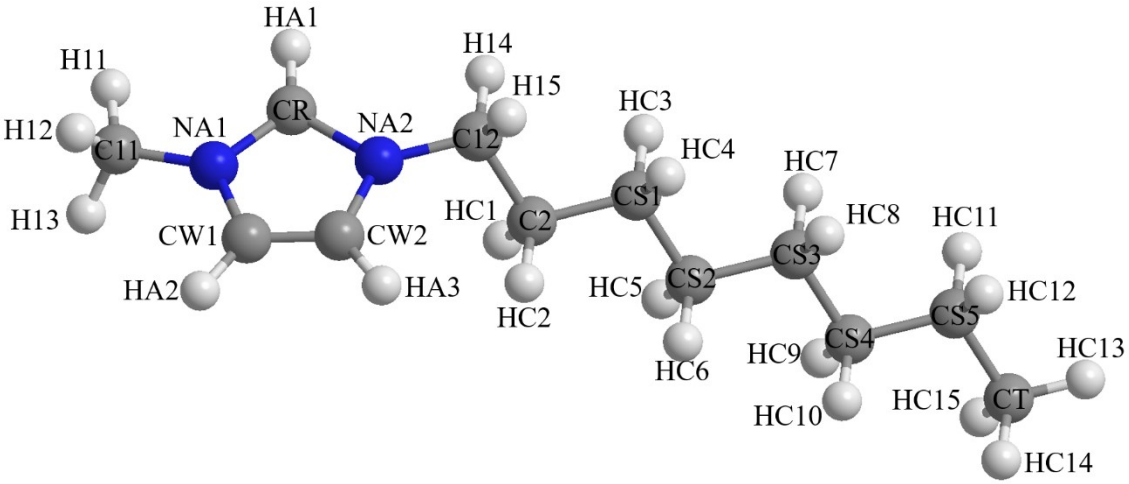

Fig. S1 Structure of $[C_8mim]^+$.

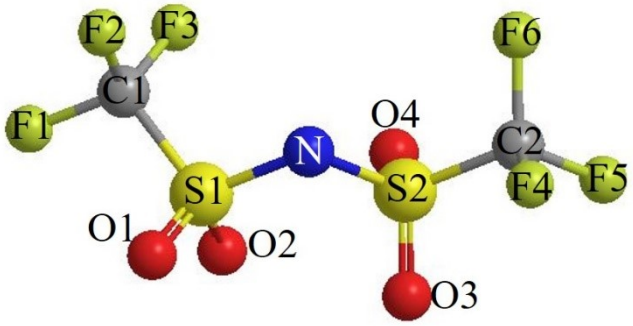

Fig. S2 Structure of $[TFSI]^-$.

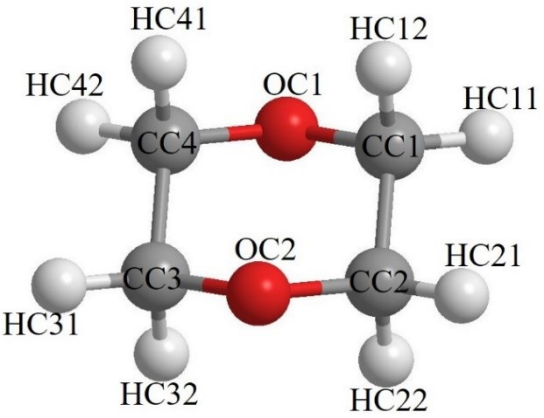

Fig. S3 Structure of 1,4-DIO.

Table S1. Atomic parameters for [C_8mim][TFSI] and 1,4-DIO.

	Atom	Charge / e	σ / Å	ε / kcal mol^{-1}
[C_8mim]$^+$	NA1	0.150	3.250	0.170
	NA2	0.150	3.250	0.170
	CR	-0.110	3.550	0.070
	HA1	0.210	2.420	0.030
	CW1	-0.130	3.550	0.070
	HA2	0.210	2.420	0.030
	CW2	-0.130	3.550	0.070
	HA3	0.210	2.420	0.030
	C11	-0.170	3.500	0.066
	H11	0.130	2.500	0.030
	H12	0.130	2.500	0.030
	H13	0.130	2.500	0.030
	C12	-0.170	3.500	0.066
	H14	0.130	2.500	0.030
	H15	0.130	2.500	0.030
	C2	0.010	3.500	0.066
	HC1	0.060	2.500	0.030
	HC2	0.060	2.500	0.030
	CS1	-0.120	3.500	0.066
	HC3	0.060	2.500	0.030
	HC4	0.060	2.500	0.030
	CS2	-0.120	3.500	0.066
	HC5	0.060	2.500	0.030
	HC6	0.060	2.500	0.030
	CS3	-0.120	3.500	0.066
	HC7	0.060	2.500	0.030
	HC8	0.060	2.500	0.030
	CS4	-0.120	3.500	0.066
	HC9	0.060	2.500	0.030
	HC10	0.060	2.500	0.030
	CS5	-0.120	3.500	0.066
	HC11	0.060	2.500	0.030
	HC12	0.060	2.500	0.030
	CT	-0.180	3.500	0.066

Cont.	HC13	0.060	2.500	0.030
	HC14	0.060	2.500	0.030
	HC15	0.060	2.500	0.030
[TFSI]$^-$	N	-0.660	3.250	0.170
	S1	1.020	3.550	0.250
	S2	1.020	3.550	0.250
	C1	0.350	3.500	0.066
	C2	0.350	3.500	0.066
	O1	-0.530	2.960	0.210
	O2	-0.53	2.960	0.210
	O3	-0.530	2.960	0.210
	O4	-0.530	2.960	0.210
	F1	-0.160	2.950	0.053
	F2	-0.16	2.950	0.053
	F3	-0.16	2.950	0.053
	F4	-0.160	2.950	0.053
	F5	-0.160	2.950	0.053
	F6	-0.160	2.950	0.053
1,4-DIO	CC1	0.140	3.500	0.066
	OC1	-0.400	2.900	0.140
	HC11	0.030	2.500	0.030
	HC12	0.030	2.500	0.030
	CC2	0.140	3.500	0.066
	OC2	-0.400	2.900	0.140
	HC21	0.030	2.500	0.030
	HC22	0.030	2.500	0.030
	CC3	0.140	3.500	0.066
	HC31	0.030	2.500	0.030
	HC32	0.030	2.500	0.030
	CC4	0.140	3.500	0.066
	HC41	0.030	2.500	0.030
	HC42	0.030	2.500	0.030

Table S2. Bond stretching parameters for [C_8mim][TFSI] and 1,4-DIO.

	Bond	*r* / Å
$[C_8mim]^+$	CR-NA1	1.315
	CR-NA2	1.315
	C11-H11	1.090
	C11-H12	1.090
	C11-H13	1.090
	NA2-C11	1.466
	CR-HA1	1.080
	CW2-NA2	1.378
	CW1-NA1	1.378
	CW2-CW1	1.341
	CW2-HA3	1.080
	CW1-HA2	1.080
	NA1-C12	1.466
	C12-H14	1.090
	C12-H15	1.090
	C12-C2	1.529
	C2-HC1	1.090
	C2-HC2	1.090
	C2-CS1	1.529
	CS1-HC3	1.090
	CS1-HC4	1.090
	CS1-CS2	1.529
	CS2-HC5	1.090
	CS2-HC6	1.090
	CS2-CS3	1.529
	CS3-HC7	1.090
	CS3-HC8	1.090
	CS3-CS4	1.529
	CS4-HC9	1.090
	CS4-HC10	1.090
	CS4-CS5	1.529
	CS5-HC11	1.090
	CS5-HC12	1.090
	CS5-CT	1.529

Cont.	CT-HC13	1.090
	CT-HC14	1.090
	CT-HC15	1.090
[TFSI]$^-$	N-S1	1.570
	N-S2	1.570
	S1-C1	1.818
	S1-O1	1.437
	S1-O2	1.437
	S2-C2	1.818
	S2-O3	1.437
	S2-O4	1.437
	C1-F1	1.323
	C1-F2	1.323
	C1-F3	1.323
	C2-F4	1.323
	C2-F5	1.323
	C2-F6	1.323
1,4-DIO	CC1-OC1	1.410
	CC1-CC2	1.529
	CC1-HC11	1.090
	CC1-HC12	1.090
	CC2-OC2	1.410
	CC2-HC21	1.090
	CC2-HC22	1.090
	CC3-OC2	1.410
	CC3-CC4	1.529
	CC3-HC31	1.090
	CC3-HC32	1.090
	CC4-OC1	1.410
	CC4-HC41	1.090
	CC4-HC42	1.090

Table S3. Angle bending parameters for [C_8mim][TFSI] and 1,4-DIO.

	Angle	K / kcal mol^{-1} rad^{-2}	θ / degree
[C_8mim]$^+$	H11-C11-H12	33.00	107.8
	H11-C11-H13	33.00	107.8
	H12-C11-H13	33.00	107.8
	NA2-C11-H11	37.50	110.7
	NA2-C11-H12	37.50	110.7
	NA2-C11-H13	37.50	110.7
	CR-NA2-C11	70.00	126.4
	CW2-NA2-C11	70.00	125.6
	NA2-CR-HA1	35.00	125.1
	NA1-CR-HA1	35.00	125.1
	NA2-CR-NA1	70.00	109.8
	CR-NA2-CW2	70.00	108.0
	CR-NA1-CW1	70.00	108.0
	NA2-CW2-CW1	70.00	107.1
	NA1-CW1-CW2	70.00	107.1
	NA1-CW2-HA3	35.00	122.0
	NA1-CW1-HA2	35.00	122.0
	CW2-CW1-HA2	35.00	130.9
	CW1-CW2-HA3	35.00	130.9
	CW2-NA1-C12	70.00	125.6
	CR-NA1-C12	70.00	126.4
	NA1-C12-H14	37.50	110.7
	NA1-C12-H15	37.50	110.7
	NA1-C12-C2	58.30	112.7
	C2-C12-H14	37.50	110.7
	C2-C12-H15	37.50	110.7
	H14-C12-H15	33.00	107.8
	C12-C2-HC1	37.50	110.7
	C12-C2-HC2	37.50	110.7
	C12-C2-CS1	58.30	112.7
	CT-CS5-HC11	37.50	110.7
	CT-CS5-HC12	37.50	110.7
	CS1-C2-HC1	37.50	110.7
	CS1-C2-HC2	37.50	110.7

Cont.	C2-CS1-HC3	37.50	110.7
	C2-CS1-HC4	37.50	110.7
	CS2-CS1-HC3	37.50	110.7
	CS2-CS1-HC4	37.50	110.7
	CS3-CS2-HC5	37.50	110.7
	CS3-CS2-HC6	37.50	110.7
	CS3-CS2-HC5	37.50	110.7
	CS3-CS2-HC6	37.50	110.7
	CS2-CS3-HC7	37.50	110.7
	CS2-CS3-HC8	37.50	110.7
	CS4-CS3-HC7	37.50	110.7
	CS4-CS3-HC8	37.50	110.7
	CS3-CS4-HC9	37.50	110.7
	CS3-CS4-HC10	37.50	110.7
	CS5-CS4-HC9	37.50	110.7
	CS5-CS4-HC10	37.50	110.7
	CS4-CS5-HC11	37.50	110.7
	CS4-CS5-HC12	37.50	110.7
	HC1-C2-HC2	33.00	107.8
	HC3-CS1-HC4	33.00	107.8
	HC5-CS2-HC6	33.00	107.8
	HC7-CS3-HC8	33.00	107.8
	HC9-CS4-HC10	33.00	107.8
	HC11-CS5-HC12	33.00	107.8
	CS4-CS5-CT	58.30	112.7
	C2-CS1-CS2	58.30	112.7
	CS1-CS2-CS3	58.30	112.7
	CS2-CS3-CS4	58.30	112.7
	CS3-CS4-CS5	58.30	112.7
	CS5-CT-HC13	37.50	110.7
	CS5-CT-HC14	37.50	110.7
	CS5-CT-HC15	37.50	110.7
	HC13-CT-HC14	33.00	107.8
	HC13-CT-HC15	33.00	107.8
	HC14-CT-HC15	33.00	107.8

Cont.

$[TFSI]^-$	N-S1-C1	91.30	103.5
	N-S1-O1	94.20	113.6
	N-S1-O2	94.20	113.6
	N-S2-C2	91.30	103.5
	N-S2-O3	94.20	113.6
	N-S2-O4	94.20	113.6
	S1-N-S3	80.10	125.6
	S1-C1-F1	82.90	111.7
	S1-C1-F2	82.90	111.7
	S1-C1-F3	82.90	111.7
	S2-C2-F4	82.90	111.7
	S2-C2-F5	82.90	111.7
	S2-C2-F6	82.90	111.7
	C1-S1-O1	103.90	102.6
	C1-S1-O2	103.90	102.6
	C2-S2-O3	103.90	102.6
	C2-S2-O4	103.90	102.6
	O1-S1-O2	115.70	118.5
	O3-S2-O4	115.70	118.5
	F1-C1-F2	93.30	107.1
	F1-C1-F3	93.30	107.1
	F2-C1-F3	93.30	107.1
	F4-C2-F5	93.30	107.1
	F4-C2-F6	93.30	107.1
	F5-C2-F6	93.30	107.1
1,4-DIO	HC11-CC1-OC1	35.00	109.5
	HC12-CC1-OC1	35.00	109.5
	CC2-CC1-OC1	50.00	109.5
	CC2-CC1-HC11	37.50	110.7
	CC2-CC1-HC12	37.50	110.7
	HC11-CC1-HC12	33.00	107.8
	CC1-CC2-OC2	50.00	109.5
	CC1-CC2-HC21	37.50	110.7
	CC1-CC2-HC22	37.50	110.7
	HC21-CC2-OC2	35.00	109.5

Cont.	HC22-CC2-OC2	35.00	109.5
	HC21-CC2-HC22	33.00	107.8
	CC2-OC2-CC3	60.00	109.5
	CC4-CC3-OC2	50.00	109.5
	HC31-CC3-OC2	35.00	109.5
	HC32-CC3-OC2	35.00	109.5
	CC4-CC3-HC31	37.50	110.7
	CC4-CC3-HC32	37.50	110.7
	HC31-CC3-HC32	33.00	107.8
	CC3-CC4-OC1	50.00	109.5
	CC3-CC4-HC41	37.50	110.7
	CC3-CC4-HC42	37.50	110.7
	HC41-CC4-OC1	35.00	109.5
	HC42-CC4-OC1	35.00	109.5
	HC41-CC4-HC42	33.00	107.8
	CC1-OC1-CC4	60.00	109.5

Table S4. Dihedral parameters for [C_8mim][TFSI] and 1,4-DIO.

	Dihedral	V_1 / kcal mol^{-1}	V_2 / kcal mol^{-1}	V_3 / kcal mol^{-1}	V_4 / kcal mol^{-1}
[C_8mim]$^+$	CR-NA2-C11-H11	0.000	0.000	0.000	0.000
	CR-NA2-C11-H12	0.000	0.000	0.000	0.000
	CR-NA2-C11-H13	0.000	0.000	0.000	0.000
	CW2-NA2-C11-H11	0.000	0.000	0.124	0.000
	CW2-NA2-C11-H12	0.000	0.000	0.124	0.000
	CW2-NA2-C11-H13	0.000	0.000	0.124	0.000
	C11-NA2-CR-HA1	0.000	4.650	0.000	0.000
	NA1-CR-NA2-C11	0.000	4.650	0.000	0.000
	CW1-CW2-NA-C11	0.000	3.000	0.000	0.000
	C11-NA2-CW2-HA3	0.000	3.000	0.000	0.000
	NA1-CR-NA2-C11	0.000	4.650	0.000	0.000
	NA2-CW2-CW1-HA2	0.000	10.750	0.000	0.000
	NA1-CW1-CW2-HA3	0.000	10.750	0.000	0.000
	NA2-CW2-CW1-NA1	0.000	10.750	0.000	0.000
	CW2-NA2-CR-HA1	0.000	4.650	0.000	0.000
	CW1-NA1-CR-HA1	0.000	4.650	0.000	0.000
	CR-NA2-CW2-HA3	0.000	3.000	0.000	0.000
	CR-NA1-CW1-HA2	0.000	3.000	0.000	0.000
	CR-NA1-CW1-CW2	0.000	3.000	0.000	0.000
	CR-NA2-CW2-CW1	0.000	3.000	0.000	0.000
	C12-NA1-CR-HA1	0.000	4.650	0.000	0.000
	C12-NA1-CW1-HA2	0.000	3.000	0.000	0.000
	C12-NA1-CW1-CW2	0.000	3.000	0.000	0.000
	CR-NA1-C12-H14	0.000	0.000	0.000	0.000
	CR-NA1-C12-H15	0.000	0.000	0.000	0.000
	C12-C2-CS1-HC3	0.000	0.000	0.366	0.000
	C12-C2-CS1-HC4	0.000	0.000	0.366	0.000
	HC1-C2-CS1-HC3	0.000	0.000	0.318	0.000
	HC1-C2-CS1-HC4	0.000	0.000	0.318	0.000
	HC2-C2-CS1-HC3	0.000	0.000	0.318	0.000
	HC2-C2-CS1-HC4	0.000	0.000	0.318	0.000
	HC3-CS1-CS2-HC5	0.000	0.000	0.318	0.000
	HC3-CS1-CS2-HC6	0.000	0.000	0.318	0.000

Cont.	HC4-CS1-CS2-HC5	0.000	0.000	0.318	0.000
	HC4-CS1-CS2-HC6	0.000	0.000	0.318	0.000
	HC5-CS2-CS3-HC7	0.000	0.000	0.318	0.000
	HC5-CS2-CS3-HC8	0.000	0.000	0.318	0.000
	HC6-CS2-CS3-HC7	0.000	0.000	0.318	0.000
	HC6-CS2-CS3-HC8	0.000	0.000	0.318	0.000
	HC7-CS3-CS4-HC9	0.000	0.000	0.318	0.000
	HC7-CS3-CS4-HC10	0.000	0.000	0.318	0.000
	HC8-CS3-CS4-HC9	0.000	0.000	0.318	0.000
	HC8-CS3-CS4-HC10	0.000	0.000	0.318	0.000
	HC9-CS4-CS5-HC11	0.000	0.000	0.318	0.000
	HC9-CS4-CS5-HC12	0.000	0.000	0.318	0.000
	HC10-CS4-CS5-HC11	0.000	0.000	0.318	0.000
	HC10-CS4-CS5-HC12	0.000	0.000	0.318	0.000
	HC11-CS5-CT-HC13	0.000	0.000	0.318	0.000
	HC11-CS5-CT-HC14	0.000	0.000	0.318	0.000
	HC11-CS5-CT-HC15	0.000	0.000	0.318	0.000
	HC12-CS5-CT-HC13	0.000	0.000	0.318	0.000
	HC12-CS5-CT-HC14	0.000	0.000	0.318	0.000
	HC12-CS5-CT-HC15	0.000	0.000	0.318	0.000
	HC9-CS4-CS5-CT	0.000	0.000	0.366	0.000
	HC10-CS4-CS5-CT	0.000	0.000	0.366	0.000
	C12-C2-CS1-CS2	1.739	-0.157	0.279	0.000
	C2-CS1-CS2-CS3	1.739	-0.157	0.279	0.000
	CS1-CS2-CS3-CS4	1.739	-0.157	0.279	0.000
	CS2-CS3-CS4-CS5	1.739	-0.157	0.279	0.000
	CS3-CS4-CS5-CT	1.739	-0.157	0.279	0.000
	CS3-CS4-CS5-HC11	0.000	0.000	0.366	0.000
	CS3-CS4-CS5-HC12	0.000	0.000	0.366	0.000
	CS2-CS3-CS4-HC9	0.000	0.000	0.366	0.000
	CS2-CS3-CS4-HC10	0.000	0.000	0.366	0.000
	CS1-CS2-CS3-HC7	0.000	0.000	0.366	0.000
	CS1-CS2-CS3-HC8	0.000	0.000	0.366	0.000
	C2-CS1-CS2-HC5	0.000	0.000	0.366	0.000
	C2-CS1-CS2-HC6	0.000	0.000	0.366	0.000
	CS2-CS1-C2-HC1	0.000	0.000	0.366	0.000
	CS2-CS1-C2-HC2	0.000	0.000	0.366	0.000

Cont.	CS3-CS2-CS1-HC3	0.000	0.000	0.366	0.000
	CS3-CS2-CS1-HC4	0.000	0.000	0.366	0.000
	CS4-CS3-CS2-HC5	0.000	0.000	0.366	0.000
	CS4-CS3-CS2-HC6	0.000	0.000	0.366	0.000
	CS5-CS4-CS3-HC7	0.000	0.000	0.366	0.000
	CS5-CS4-CS3-HC8	0.000	0.000	0.366	0.000
	CS4-CS5-CT-HC13	0.000	0.000	0.366	0.000
	CS4-CS5-CT-HC14	0.000	0.000	0.366	0.000
	CS4-CS5-CT-HC15	0.000	0.000	0.366	0.000
	HA3-CW2-CW1-HA2	0.000	10.750	0.000	0.000
	CW1-NA1-C12-H14	0.000	0.000	0.124	0.000
	CW1-NA1-C12-H15	0.000	0.000	0.124	0.000
	CW1-NA1-C12-C2	-1.709	1.459	0.190	0.000
	CR-NA1-C12-C2	-1.259	0.000	0.000	0.000
	NA1-C12-C2-CS1	-1.787	0.756	-0.287	0.000
	H14-C12-C2-HC1	0.000	0.000	0.318	0.000
	H14-C12-C2-HC2	0.000	0.000	0.318	0.000
	H15-C12-C2-HC1	0.000	0.000	0.318	0.000
	H15-C12-C2-HC2	0.000	0.000	0.318	0.000
	NA1-C12-C2-HC1	0.000	0.000	0.088	0.000
	NA1-C12-C2-HC2	0.000	0.000	0.088	0.000
	CS1-C2-C12-HC14	0.000	0.000	0.366	0.000
	CS1-C2-C12-HC15	0.000	0.000	0.366	0.000
	NA1-CR-NA2-CW2	0.000	4.650	0.000	0.000
	NA2-CR-NA1-CW1	0.000	4.650	0.000	0.000
$[TFSI]^-$	N-S1-C1-F1	0.000	0.000	0.316	0.000
	N-S1-C1-F2	0.000	0.000	0.316	0.000
	N-S1-C1-F3	0.000	0.000	0.316	0.000
	N-S2-C2-F4	0.000	0.000	0.316	0.000
	N-S2-C2-F5	0.000	0.000	0.316	0.000
	N-S2-C2-F6	0.000	0.000	0.316	0.000
	S1-N-S2-C2	7.829	-2.489	-0.763	0.000
	S1-N-S2-O3	0.000	0.000	-0.003	0.000
	S1-N-S2-O4	0.000	0.000	-0.003	0.000
	S2-N-S1-C1	7.829	-2.489	-0.763	0.000
	S2-N-S1-O1	0.000	0.000	-0.003	0.000

Cont.	S2-N-S1-O2	0.000	0.000	-0.003	0.000
	O1-S1-C1-F1	0.000	0.000	0.347	0.000
	O1-S1-C1-F2	0.000	0.000	0.347	0.000
	O1-S1-C1-F3	0.000	0.000	0.347	0.000
	O2-S1-C1-F1	0.000	0.000	0.347	0.000
	O2-S1-C1-F2	0.000	0.000	0.347	0.000
	O2-S1-C1-F3	0.000	0.000	0.347	0.000
	O3-S2-C2-F4	0.000	0.000	0.347	0.000
	O3-S2-C2-F5	0.000	0.000	0.347	0.000
	O3-S2-C2-F6	0.000	0.000	0.347	0.000
	O4-S2-C2-F4	0.000	0.000	0.347	0.000
	O4-S2-C2-F5	0.000	0.000	0.347	0.000
	O4-S2-C2-F6	0.000	0.000	0.347	0.000
1,4-DIO	CC2-CC1-OC1-CC4	0.650	-0.250	0.670	0.000
	CC4-OC1-CC1-HC11	0.000	0.000	0.760	0.000
	CC4-OC1-CC1-HC12	0.000	0.000	0.760	0.000
	OC1-CC1-CC2-OC2	-0.550	0.000	0.000	0.000
	HC21-CC2-CC1-OC1	0.000	0.000	0.468	0.000
	HC22-CC2-CC1-OC1	0.000	0.000	0.468	0.000
	HC11-CC1-CC2-OC2	0.000	0.000	0.468	0.000
	HC11-CC1-CC2-HC21	0.000	0.000	0.300	0.000
	HC11-CC1-CC2-HC22	0.000	0.000	0.300	0.000
	HC12-CC1-CC2-OC2	0.000	0.000	0.468	0.000
	HC12-CC1-CC2-HC21	0.000	0.000	0.300	0.000
	HC12-CC1-CC2-HC22	0.000	0.000	0.300	0.000
	CC1-CC2-OC2-CC3	0.650	-0.250	0.670	0.000
	CC3-OC2-CC2-HC21	0.000	0.000	0.760	0.000
	CC3-OC2-CC2-HC22	0.000	0.000	0.760	0.000
	CC4-CC3-OC2-CC2	0.650	-0.250	0.670	0.000
	CC2-OC2-CC3-HC31	0.000	0.000	0.760	0.000
	CC2-OC2-CC3-HC32	0.000	0.000	0.760	0.000
	OC2-CC3-CC4-OC1	-0.550	0.000	0.000	0.000
	HC41-CC4-CC3-OC2	0.000	0.000	0.468	0.000
	HC42-CC4-CC3-OC2	0.000	0.000	0.468	0.000
	HC31-CC3-CC4-OC1	0.000	0.000	0.468	0.000
	HC31-CC3-CC4-HC41	0.000	0.000	0.300	0.000

Cont.	HC31-CC3-CC4-HC42	0.000	0.000	0.300	0.000
	HC32-CC3-CC4-OC1	0.000	0.000	0.468	0.000
	HC32-CC3-CC4-HC41	0.000	0.000	0.300	0.000
	HC32-CC3-CC4-HC42	0.000	0.000	0.300	0.000
	CC3-CC4-OC1-CC1	0.650	-0.250	0.670	0.000
	CC1-OC1-CC4-HC41	0.000	0.000	0.760	0.000
	CC1-OC1-CC4-HC42	0.000	0.000	0.760	0.000

Table. S5 Densities of d_{MD} derived from MD simulations and d_{exp} experimentally determined, and the deviation of Δd, respectively.[a]

$x_{1,4\text{-DIO}}$	T / K	d_{MD} / g cm^{-3}	d_{exp} / g cm^{-3}	Δd / %
0 (neat IL)	308.2	1.369	1.312	4.3
	313.2	1.365	1.307	4.4
	323.2	1.358	1.299	4.5
	333.2	1.348	1.290	4.5
	343.2		1.281	
	348.2	1.334		
	373.2	1.310		
0.983	308.2	1.025	1.037	-1.2
	313.2	1.019	1.031	-1.2
	323.2	1.006	1.021	-1.5
	333.2	0.9932	1.010	-1.7
	343.2		0.9983	
	348.2	0.9734		
	373.2	0.9396		
1	308.2	1.001	1.017	-1.6
	313.2	0.9938	1.011	-1.7
	323.2	0.9813	0.9995	-1.8
	333.2	0.9684	0.9881	-2.0
	343.2		0.9766	
	348.2	0.9483		
	373.2	0.9143		

[a] Calculation for MD simulations at 343.2 K was not performed.

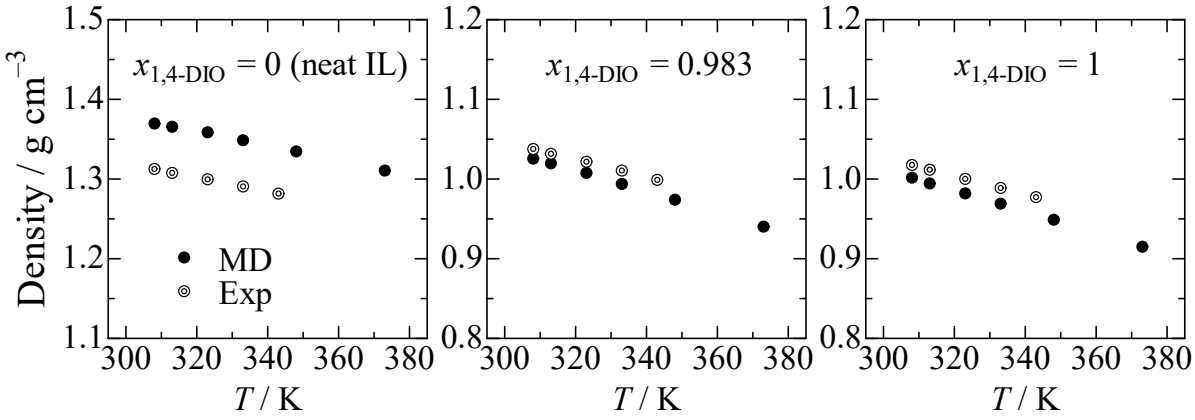

Fig. S4 Simulated and experimental densities for [C_8mim][TFSI]–1,4-DIO system at $x_{1,4\text{-DIO}}$ = 0 (neat IL) (left), $x_{1,4\text{-DIO}}$ = 0.983 (middle), and $x_{1,4\text{-DIO}}$ = 1 (right), as a function of temperature.

Table S6. Phase separation points in the liquid-liquid phase diagrams (Fig. 2) of [$C_n$mim][TFSI]–1,4-DIO and [C_8mim][TFSI]–1,4-DIO-d_8 systems.

n = 2		n = 4		n = 6		n = 8		n = 8 (1,4-DIO-d_8)	
$x_{1,4\text{-DIO}}$	T / K	$x_{1,4\text{-DIO}}$	T / K	$x_{1,4\text{-DIO}}$	T / K	$x_{1,4\text{-DIO}}$	T / K	$x_{1,4\text{-DIO-}d8}$	T / K
0.8775	290.2	0.8978	285.8	0.9299	295.6	0.9549	290.3	0.9600	294.1
0.8790	296.8	0.8996	290.4	0.9401	312.4	0.9574	292.8	0.9700	301.6
0.8797	300.4	0.9028	298.4	0.9503	323.5	0.9599	294.9	0.9760	304.1
0.8809	306.2	0.9068	306.0	0.9598	334.0	0.9624	297.2	0.9822	304.2
0.8827	315.1	0.9075	311.0	0.9652	337.2	0.9650	299.4	0.9859	304.3
0.8844	325.9	0.9099	315.6	0.9698	338.1	0.9676	301.3	0.9901	301.8
0.8865	336.8	0.9126	323.1	0.9743	338.8	0.9701	302.4		
0.8882	344.6	0.9150	332.1	0.9800	339.2	0.9724	303.2		
0.8900	357.0	0.9201	343.4	0.9850	338.5	0.9751	303.9		
0.9975	363.4	0.9250	354.6	0.9899	336.4	0.9776	304.3		
0.9980	345.7	0.9301	366.6	0.9925	332.3	0.9801	304.6		
0.9985	318.1	0.9954	362.9	0.9949	321.5	0.9825	304.8		
		0.9960	355.0	0.9975	293.2	0.9849	304.3		
		0.9965	345.6			0.9874	303.9		
		0.9968	339.1			0.9898	302.5		
		0.9973	327.6			0.9925	299.9		
		0.9981	307.6			0.9950	291.5		

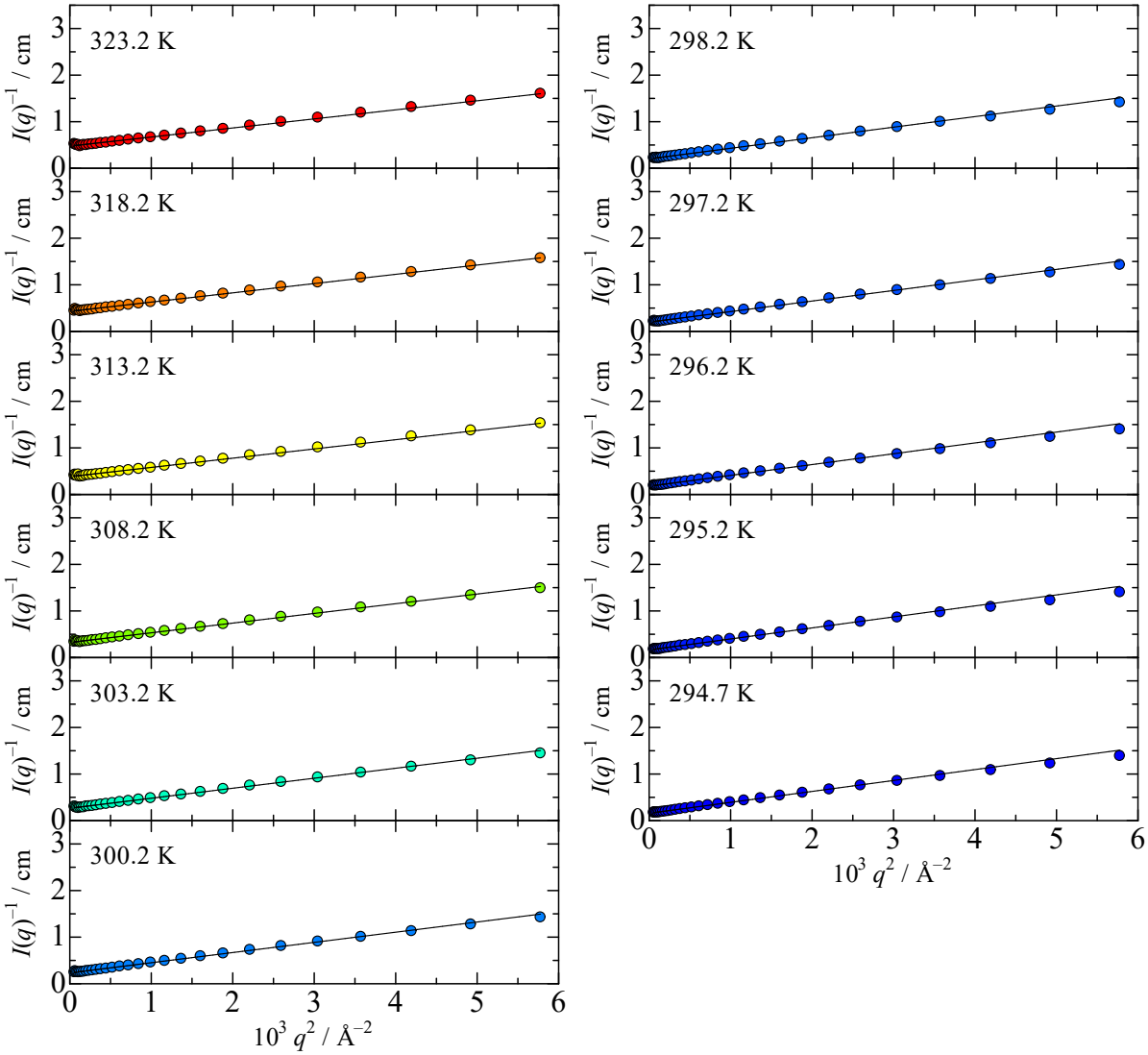

Fig. S5 $I(q)^{-1}$ plot for [C_8mim][TFSI]–1,4-DIO-d_8 solution at $x_{1,4\text{-DIO-}d8}$ = 0.960 as a function of q^2. The solid lines show the results of the Ornstein–Zernike fits.

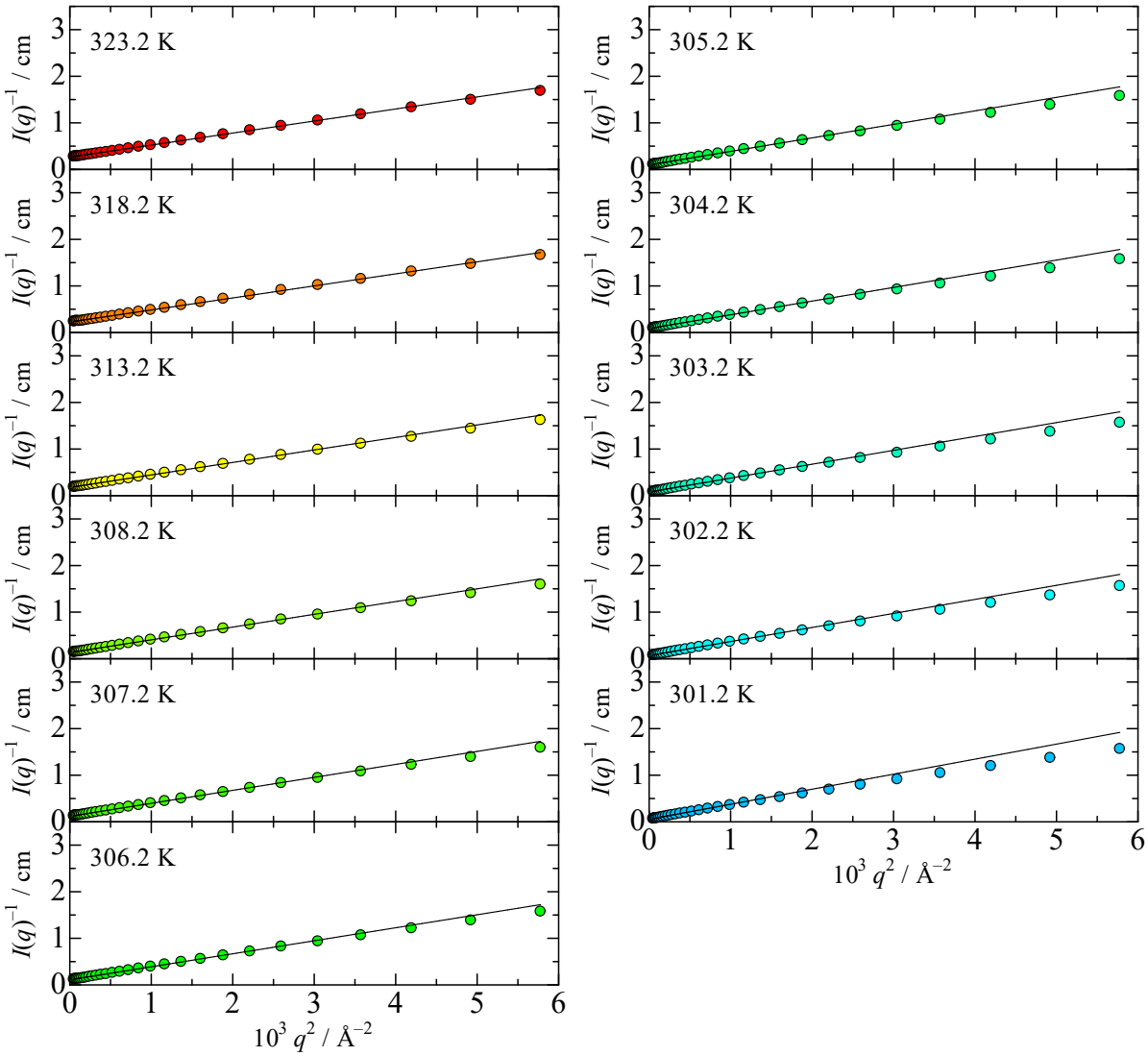

Fig. S6 $I(q)^{-1}$ plot for [C_8mim][TFSI]−1,4-DIO-d_8 solution at $x_{1,4\text{-DIO-}d8}$ = 0.970 as a function of q^2. The solid lines show the results of the Ornstein–Zernike fits.

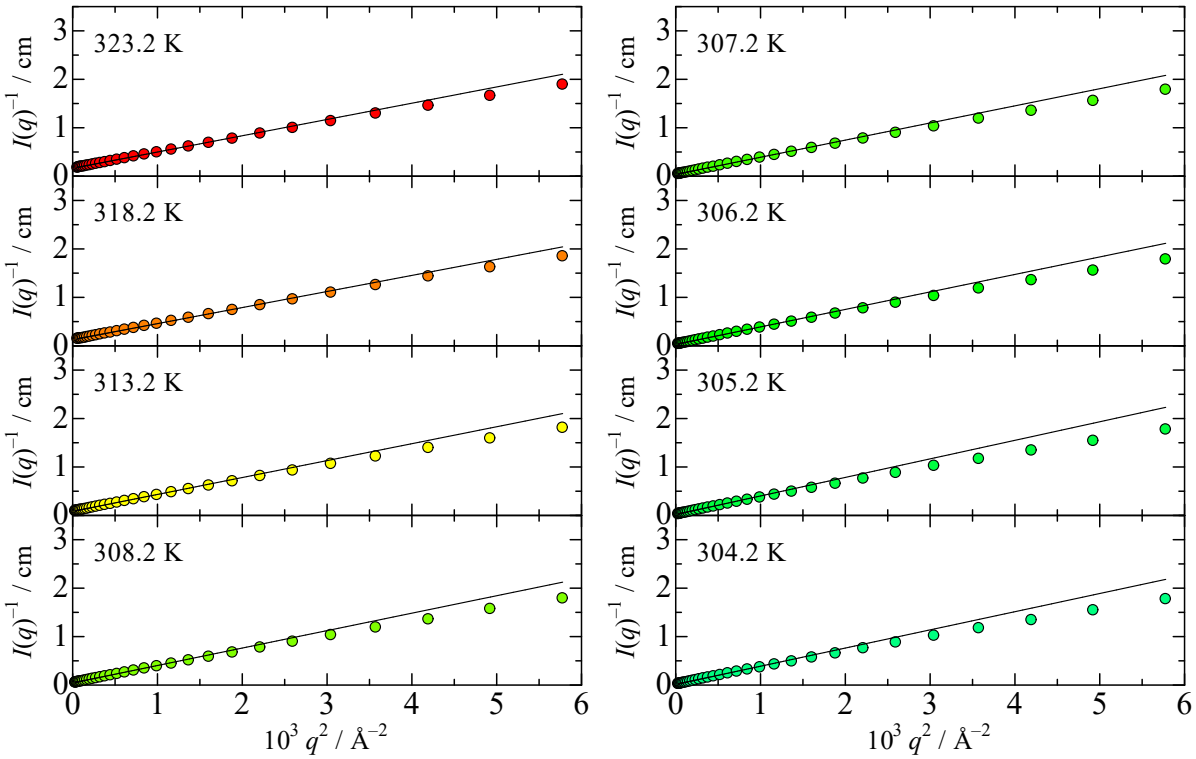

Fig. S7 $I(q)^{-1}$ plot for [C_8mim][TFSI]–1,4-DIO-d_8 solution at $x_{1,4\text{-DIO-}d8}$ = 0.976 as a function of q^2. The solid lines show the results of the Ornstein–Zernike fits.

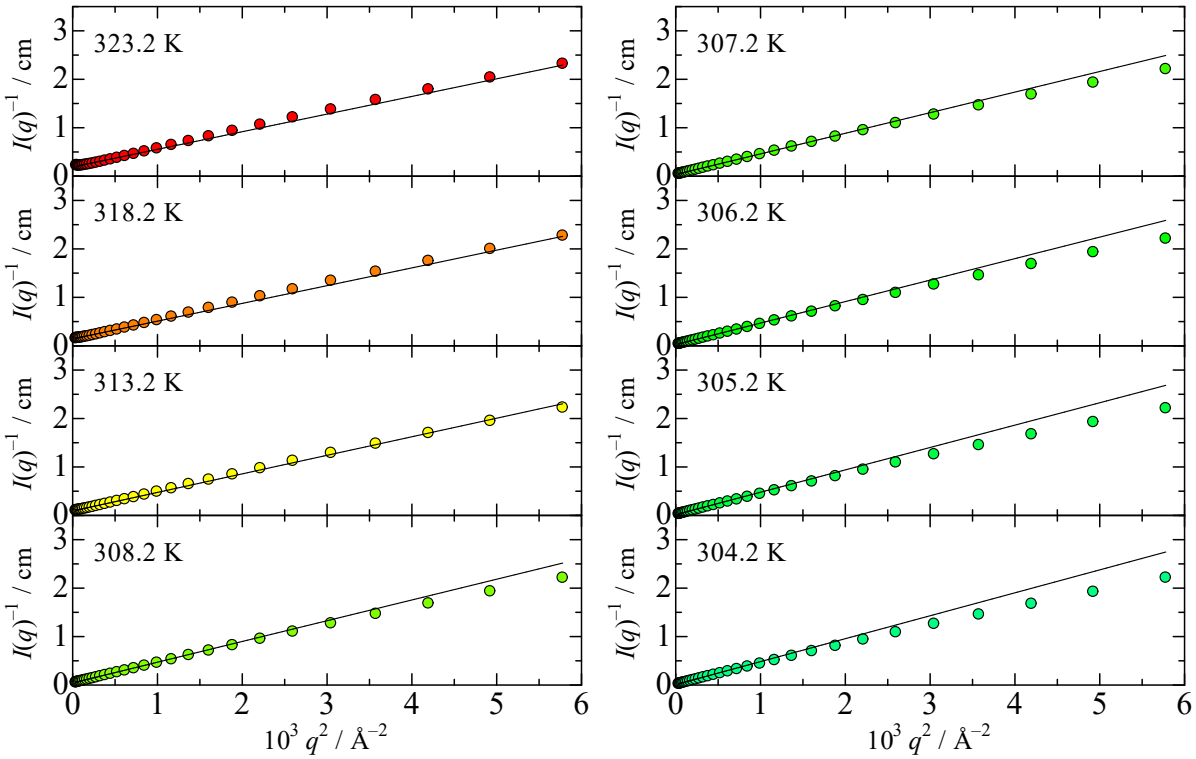

Fig. S8 $I(q)^{-1}$ plot for [C_8mim][TFSI]–1,4-DIO-d_8 solution at $x_{1,4\text{-DIO-}d8}$ = 0.982 as a function of q^2. The solid lines show the results of the Ornstein–Zernike fits.

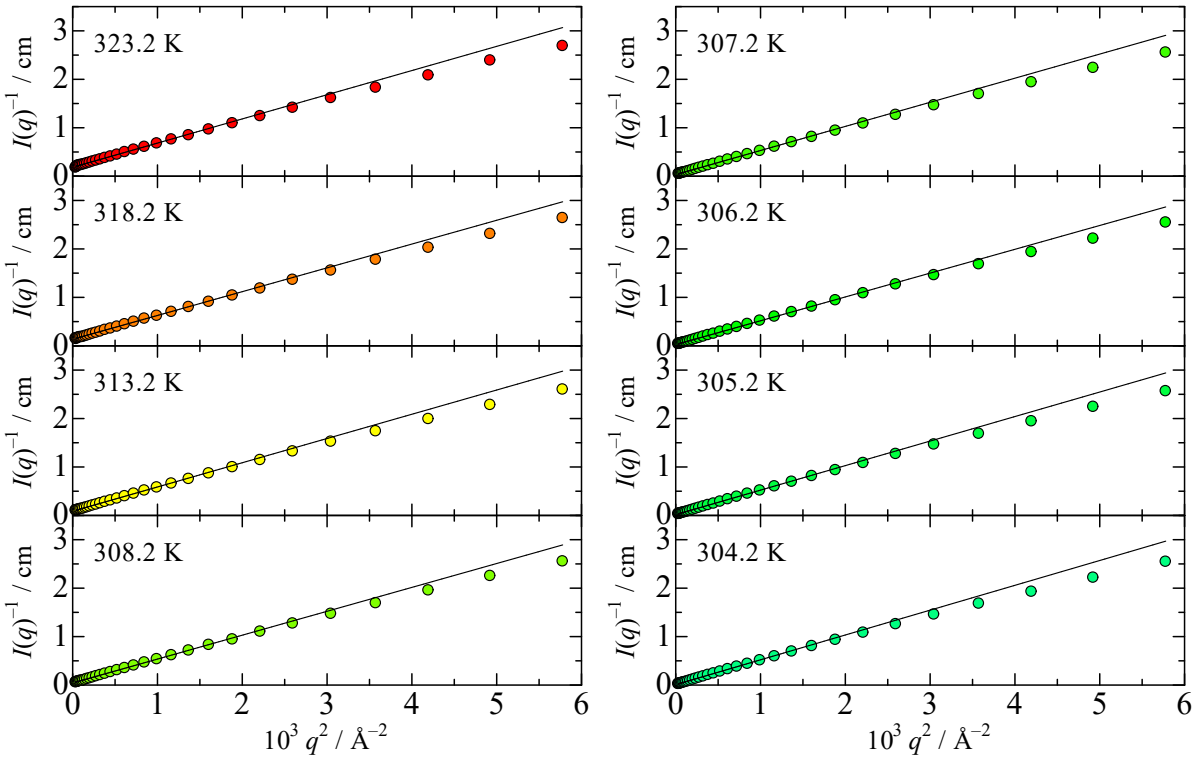

Fig. S9 $I(q)^{-1}$ plot for [C_8mim][TFSI]–1,4-DIO-d_8 solution at $x_{1,4\text{-DIO-}d8}$ = 0.986 as a function of q^2. The solid lines show the results of the Ornstein–Zernike fits.

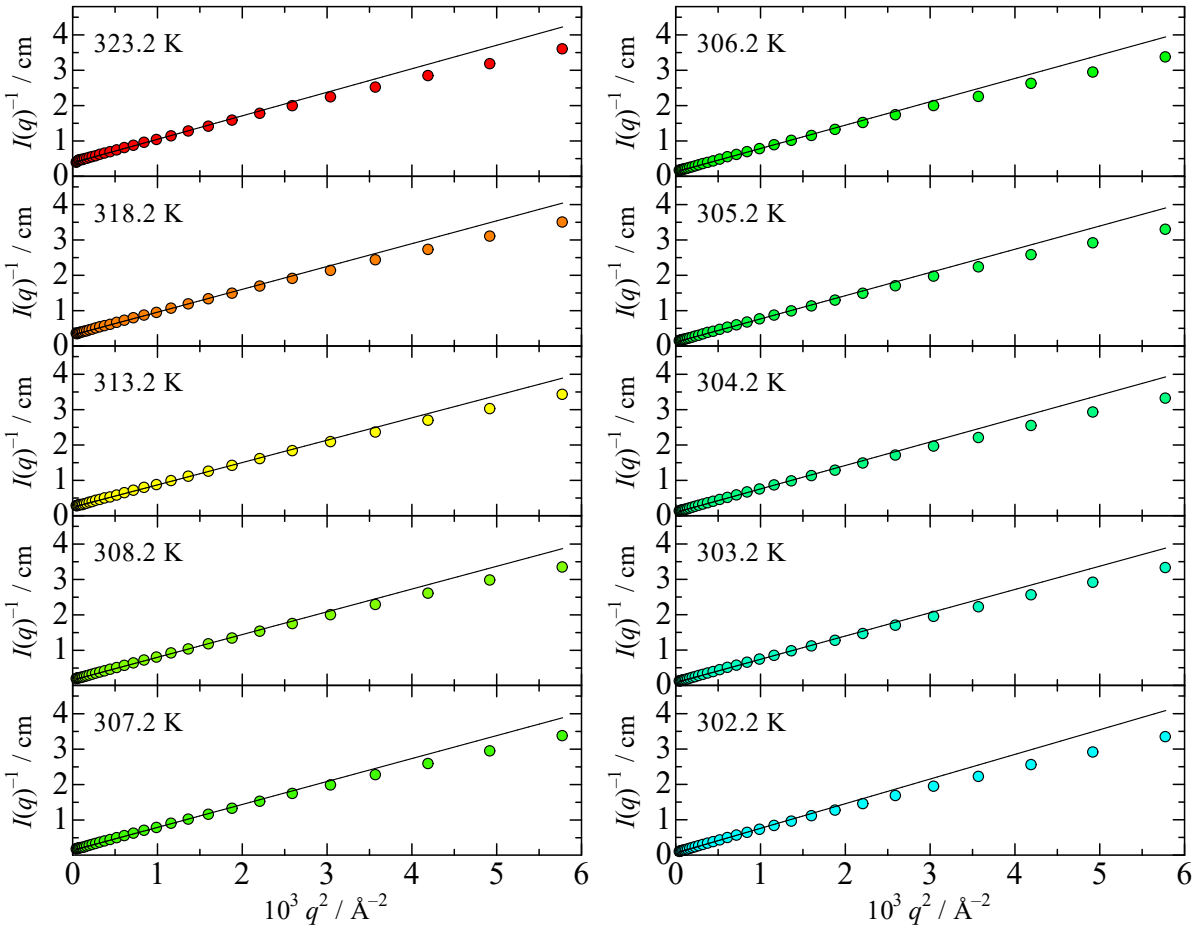

Fig. S10 $I(q)^{-1}$ plot for [C_8mim][TFSI]–1,4-DIO-d_8 solution at $x_{1,4\text{-DIO-}d8}$ = 0.990 as a function of q^2. The solid lines show the results of the Ornstein–Zernike fits.

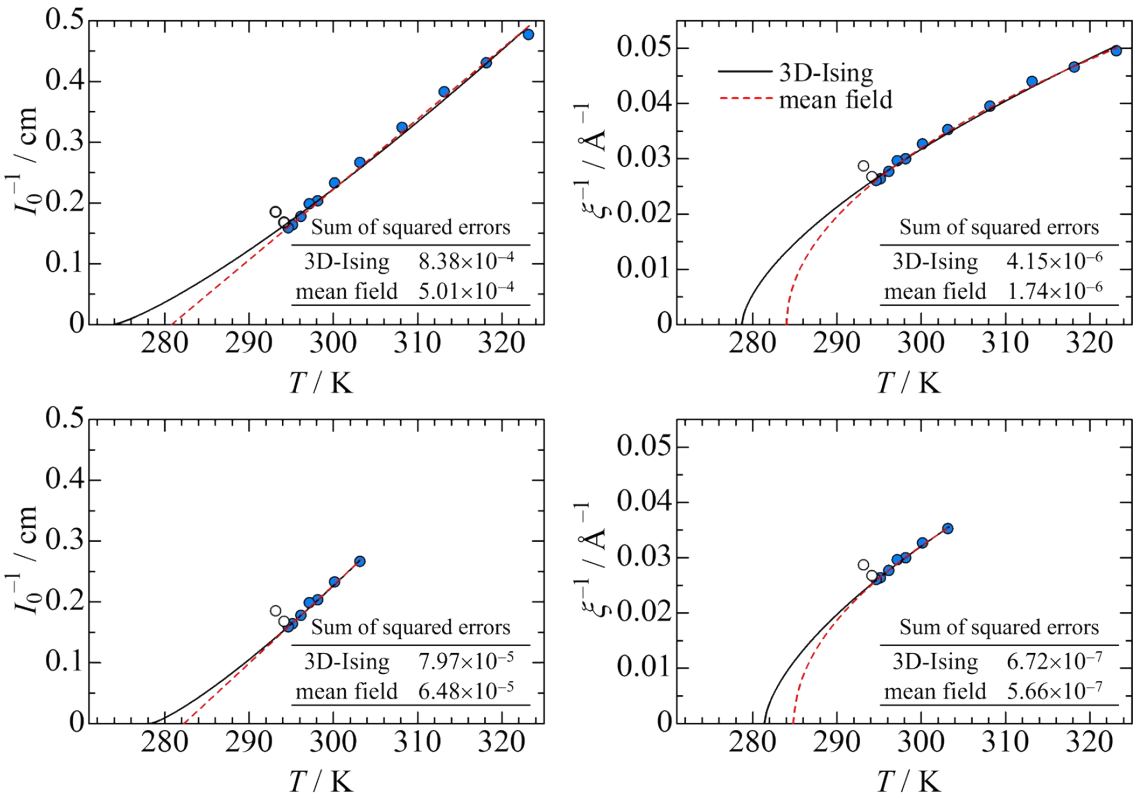

Fig. S11 Fitting for I_0^{-1} and ξ^{-1} values of [C_8mim][TFSI]–1,4-DIO-d_8 solution at $x_{1,4\text{-DIO-}d8}$ = 0.960 against T in the whole range examined (upper) and the partial range near phase separation temperature (lower panels). Solid and dashed lines show the results of fits with the assumption of 3D-Ising and mean field models, respectively, using eqns (5) and (6). White circles give the values estimated from SANS profiles for the sample solution after phase separation and were not used for the fits to determine T_s. The sums of squared errors of the fits by eqns (5) and (6) are inserted in the figures.

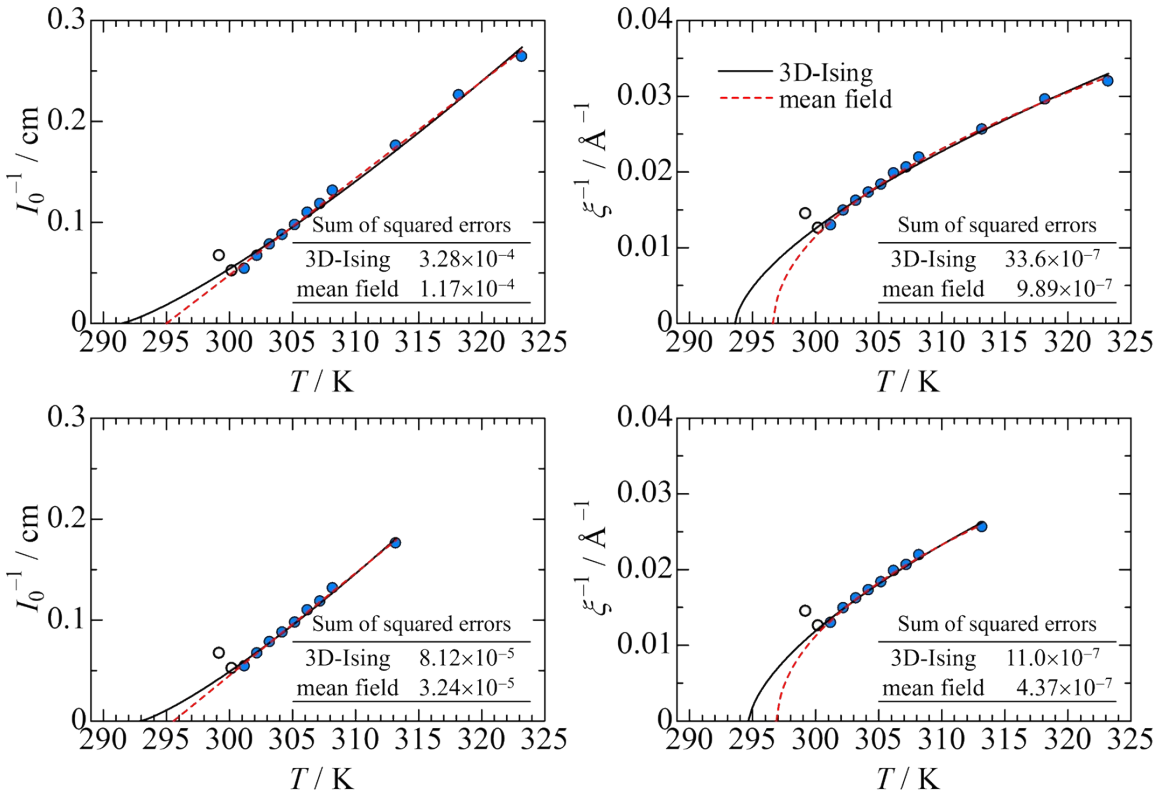

Fig. S12 Fitting for I_0^{-1} and ξ^{-1} values of [C_8mim][TFSI]–1,4-DIO-d_8 solution at $x_{1,4\text{-DIO-}d8}$ = 0.970 against T in the whole range examined (upper) and the partial range near phase separation temperature (lower panels). The types of lines and circles are the same as those in Fig. S11.

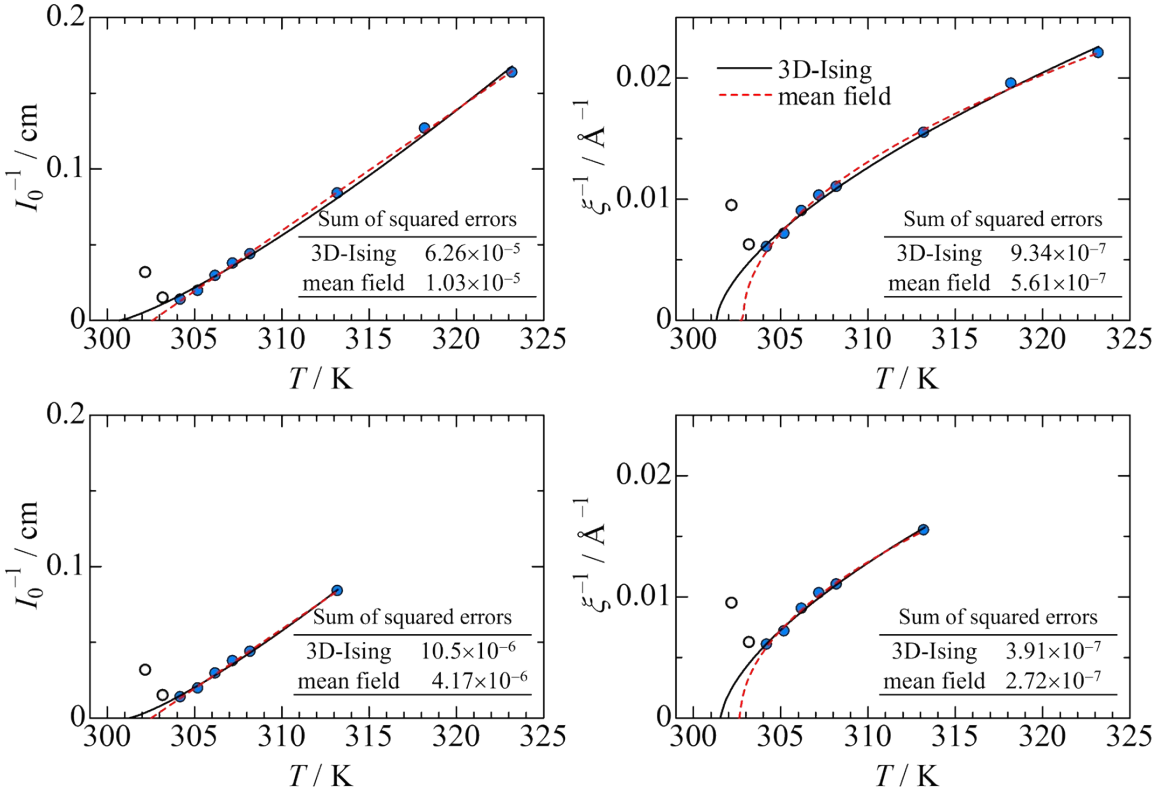

Fig. S13 Fitting for I_0^{-1} and ξ^{-1} values of [C_8mim][TFSI]–1,4-DIO-d_8 solution at $x_{1,4\text{-DIO-}d8}$ = 0.976 against T in the whole range examined (upper) and the partial range near phase separation temperature (lower panels). The types of lines and circles are the same as those in Fig. S11.

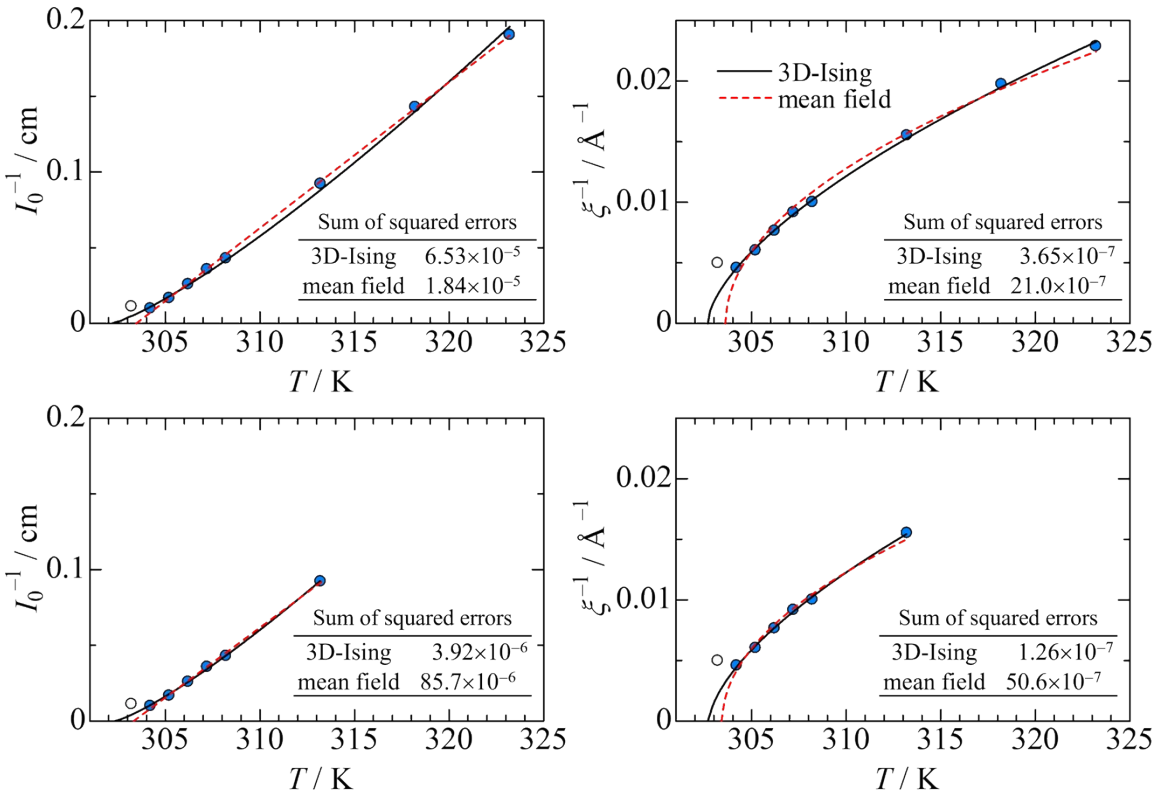

Fig. S14 Fitting for I_0^{-1} and ξ^{-1} values of [C_8mim][TFSI]–1,4-DIO-d_8 solution at $x_{1,4\text{-DIO-}d8}$ = 0.982 against T in the whole range examined (upper) and the partial range near phase separation temperature (lower panels). The types of lines and circles are the same as those in Fig. S11.

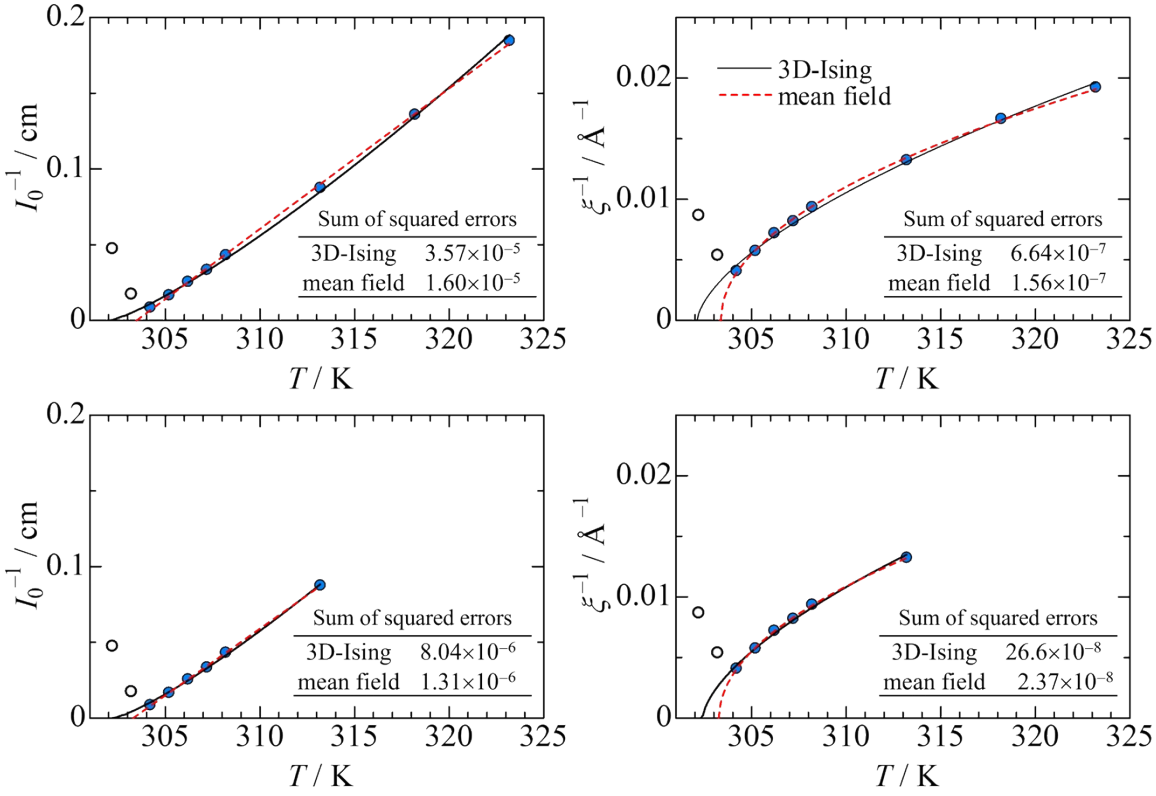

Fig. S15 Fitting for I_0^{-1} and ξ^{-1} values of [C_8mim][TFSI]–1,4-DIO-d_8 solution at $x_{1,4\text{-DIO-}d8}$ = 0.986 against T in the whole range examined (upper) and the partial range near phase separation temperature (lower panels). The types of lines and circles are the same as those in Fig. S11.

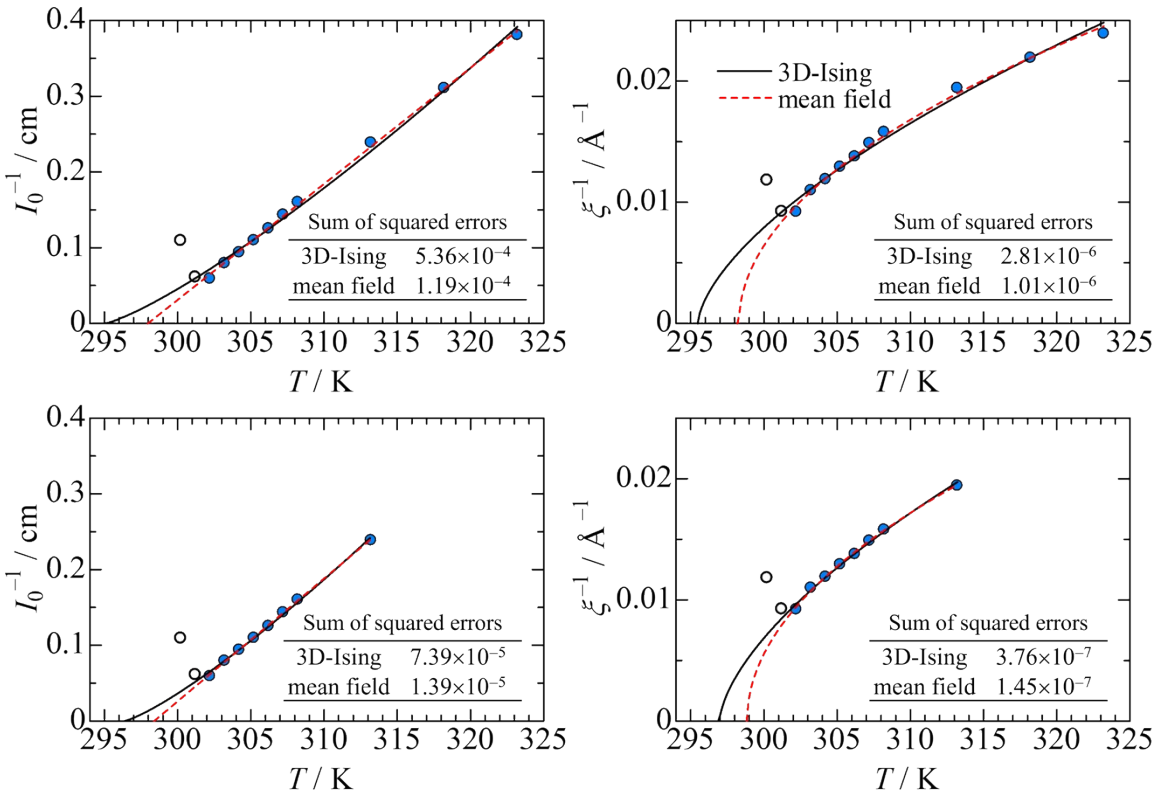

Fig. S16 Fitting for I_0^{-1} and ξ^{-1} values of [C_8mim][TFSI]–1,4-DIO-d_8 solution at $x_{1,4\text{-DIO-}d8}$ = 0.990 against T in the whole range examined (upper) and the partial range near phase separation temperature (lower panels). The types of lines and circles are the same as those in Fig. S11.

Table S7. Critical exponents of γ and ν determined from fits on I_0 and ξ values of [C_8mim][TFSI]–1,4-DIO-d_8 solutions at various $x_{1,4\text{-DIO-}d8}$, respectively, with T_s estimated from the whole T range of Figs. S11–S16. Differences give the values between the estimated critical exponents and the typical ones of γ(1.24 and 1) and ν(0.63 and 0.5). Suitability refers to which model better explains the I_0 and ξ values when comparing the results of Cases 1 and 2. The description of the model's name indicates the better explanation.

Case 1: T_s values estimated by assuming 3D-Ising model were used.

$x_{1,4\text{-DIO-}d8}$	T range / K	$T_{s\ 3D\text{-}Ising}$ / K	γ	Difference from 1.24	ν	Difference from 0.63	Suitability
0.960	294.7–323.2	276.3	1.24	0	0.72	0.09	
0.970	301.2–323.2	292.5	1.30	0.06	0.72	0.09	
0.976	304.2–323.2	301.0	1.35	0.11	0.69	0.06	
0.982	304.2–323.2	302.4	1.25	0.01	0.67	0.04	3D-Ising
0.986	304.2–323.2	302.1	1.42	0.18	0.68	0.05	
0.990	302.2–323.2	295.3	1.38	0.14	0.69	0.06	

Case 2: T_s values estimated by assuming mean field model were used.

$x_{1,4\text{-DIO-}d8}$	T range / K	$T_{s\ mean\ field}$ / K	γ	Difference from 1	ν	Difference from 0.5	Suitability
0.960	294.7–323.2	282.4	0.94	-0.06	0.55	0.05	mean field
0.970	301.2–323.2	295.8	0.99	-0.01	0.56	0.06	mean field
0.976	304.2–323.2	302.7	0.95	-0.05	0.50	0	mean field
0.982	304.2–323.2	303.5	0.83	-0.17	0.47	-0.03	
0.986	304.2–323.2	303.4	0.95	-0.05	0.48	-0.02	mean field
0.990	302.2–323.2	298.1	1.04	0.04	0.51	0.01	mean field

Table S8. Critical exponents of γ and ν determined from fits on I_0 and ξ values of [C_8mim][TFSI]–1,4-DIO-d_8 solutions at various $x_{1,4\text{-DIO-}d8}$, respectively, with T_s estimated from the partial T range of Figs. S11–S16. Differences give the values between the estimated critical exponents and the typical ones of γ(1.24 and 1) and ν(0.63 and 0.5). Suitability refers to which model better explains the I_0 and ξ values when comparing the results of Cases 3 and 4. The description of the model's name indicates the better explanation.

Case 3: T_s values estimated by assuming 3D-Ising model were used.

$x_{1,4\text{-DIO-}d8}$	T range / K	$T_{s\ 3D\text{-}Ising}$ / K	γ	Difference from 1.24	ν	Difference from 0.63	Suitability
0.960	294.7–323.2	279.9	1.17	-0.07	0.69	0.06	
0.970	301.2–323.2	293.8	1.25	0.01	0.72	0.09	
0.976	304.2–323.2	301.4	1.31	0.07	0.68	0.05	
0.982	304.2–323.2	302.5	1.22	-0.02	0.66	0.03	3D-Ising
0.986	304.2–323.2	302.3	1.41	0.17	0.70	0.07	
0.990	302.2–313.2	296.7	1.29	0.05	0.67	0.04	

Case 4: T_s values estimated by assuming mean field model were used.

$x_{1,4\text{-DIO-}d8}$	T range / K	$T_{s\ mean\ field}$ / K	γ	Difference from 1	ν	Difference from 0.5	Suitability
0.960	294.7–303.2	283.6	0.93	-0.07	0.55	0.05	mean field
0.970	301.2–313.2	296.3	0.96	-0.04	0.55	0.05	mean field
0.976	304.2–313.2	302.6	0.95	-0.05	0.50	0	mean field
0.982	304.2–313.2	303.4	0.84	-0.16	0.47	-0.03	
0.986	304.2–313.2	303.4	0.90	-0.10	0.46	-0.04	mean field
0.990	302.2–313.2	298.6	0.99	-0.01	0.52	0.02	mean field

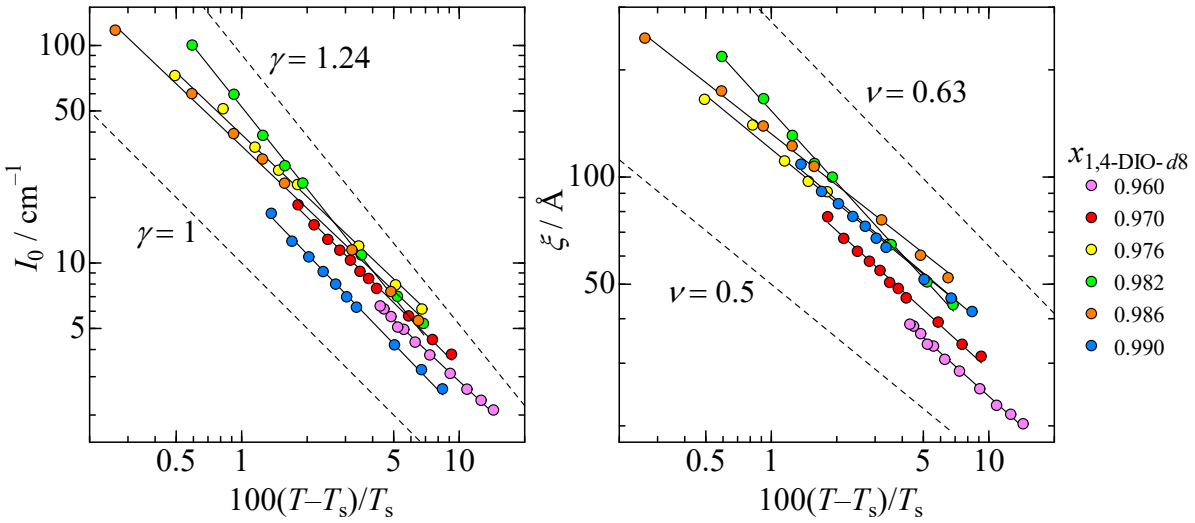

Fig. S17 γ and ν determined by fits for I_0 and ξ values of [C_8mim][TFSI]–1,4-DIO-d_8 solutions at $x_{1,4\text{-DIO-}d8}$ = 0.960, 0.970, 0.976, 0.982, 0.986 and 0.990. The dashed lines show the slopes of the typical γ (1.24 and 1, respectively) and ν (0.63 and 0.5, respectively) values for 3D-Ising and mean field.

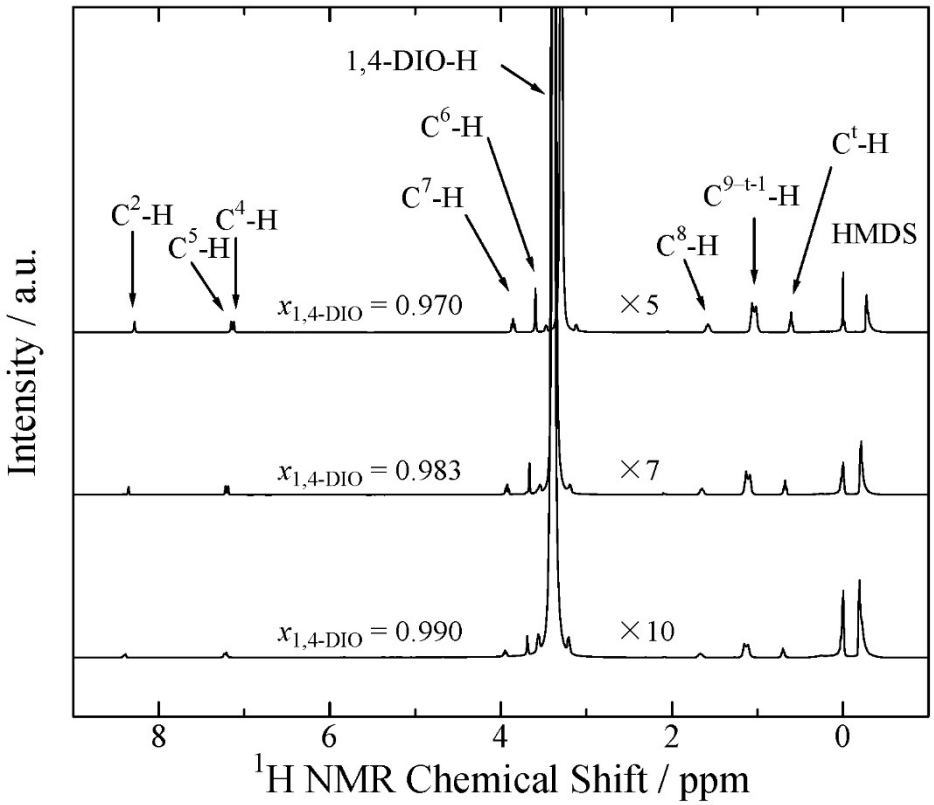

Fig. S18 ^{1}H NMR spectra of [C_8mim][TFSI]–1,4-DIO solutions at 323.2 K as a function of $x_{1,4\text{-DIO}}$.

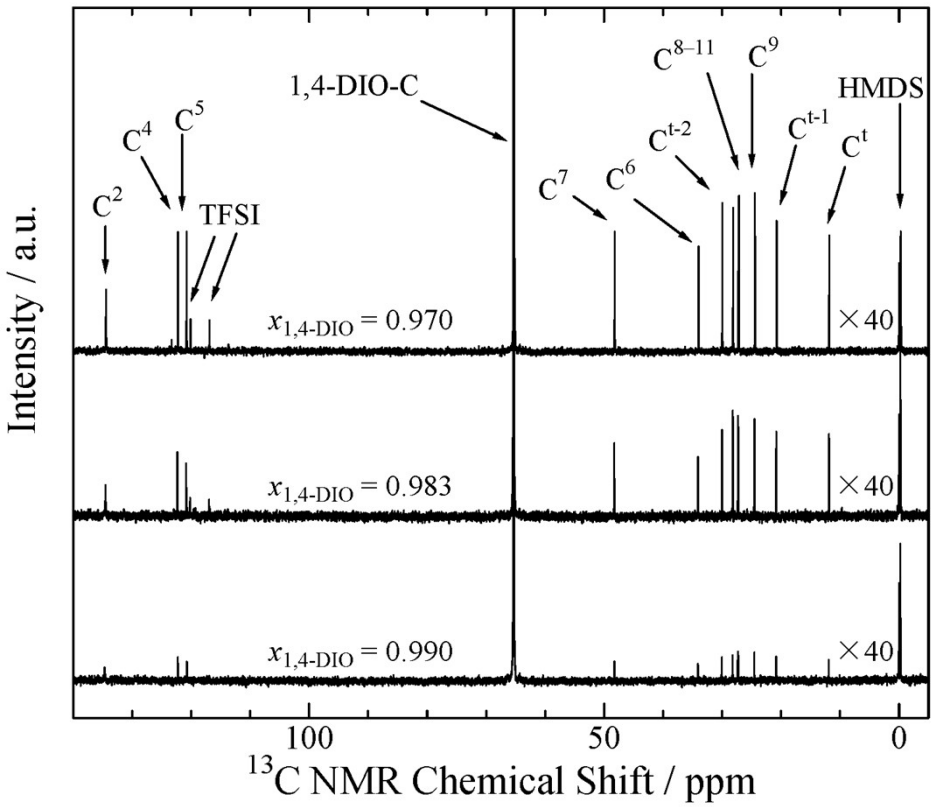

Fig. S19 ^{13}C NMR spectra of [C_8mim][TFSI]–1,4-DIO solutions at 323.2 K as a function of $x_{1,4\text{-DIO}}$.

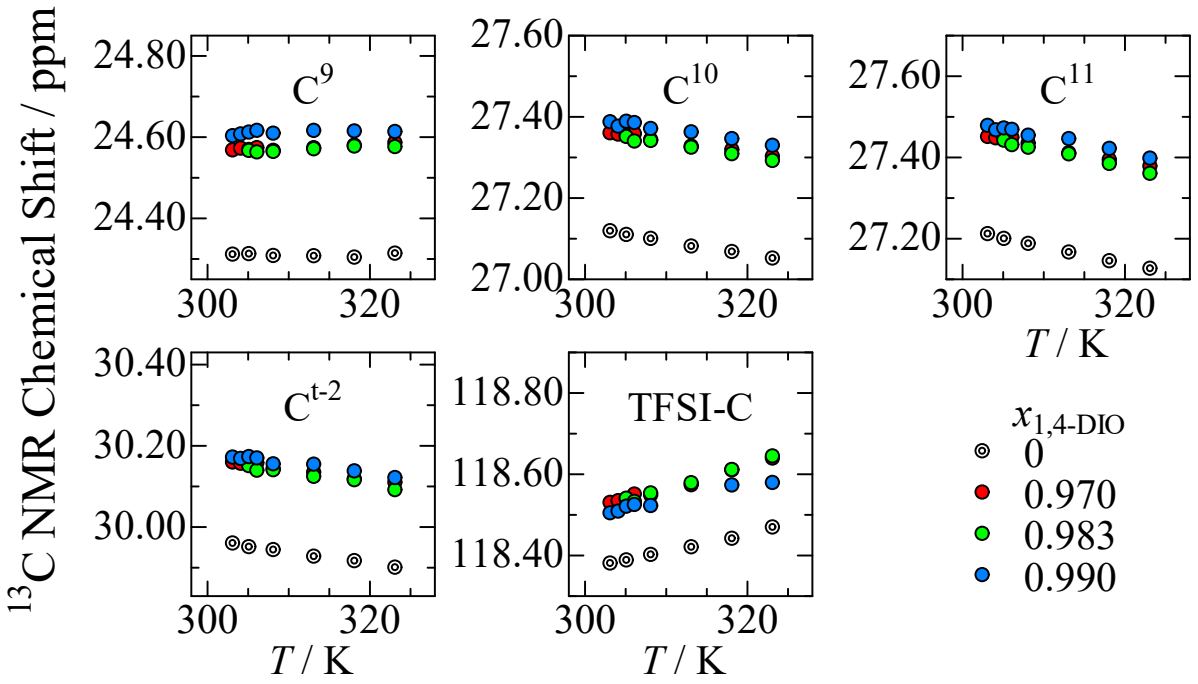

Fig. S20 ^{13}C NMR chemical shifts of $[C_8mim]^+$ and $[TFSI]^-$ in $[C_8mim][TFSI]$–1,4-DIO solutions at $x_{1,4\text{-DIO}}$ = 0, 0.970, 0.983, and 0.990 as a function of temperature before phase separation. The standard deviations σ are within ±0.009 ppm.

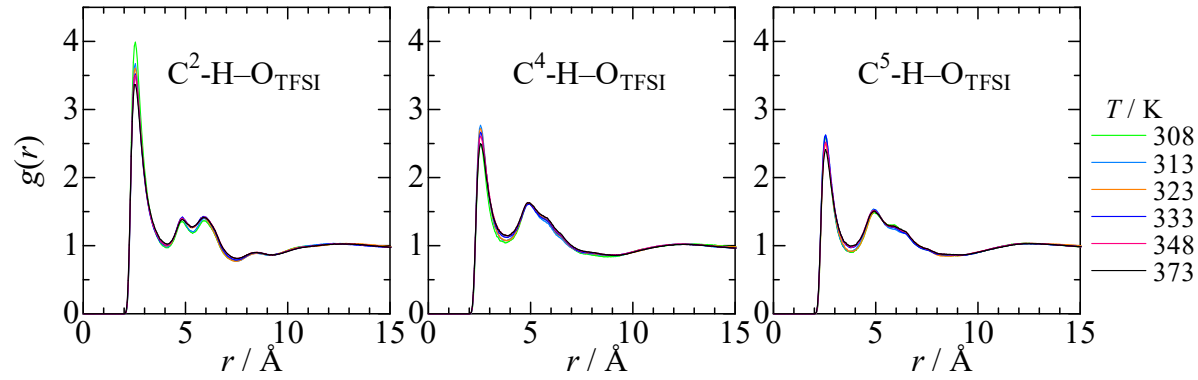

Fig. S21 Temperature dependence of MD pair correlation functions, $g(r)$s, for the $C^{2,4,5}$-H–O_{TFSI} interactions in neat $[C_8mim][TFSI]$ system ($x_{1,4\text{-DIO}}$ = 0). The $g(r)$s of the $C^{2,4,5}$-H–O_{TFSI} interactions were calculated for one of the four O atoms within $[TFSI]^-$.

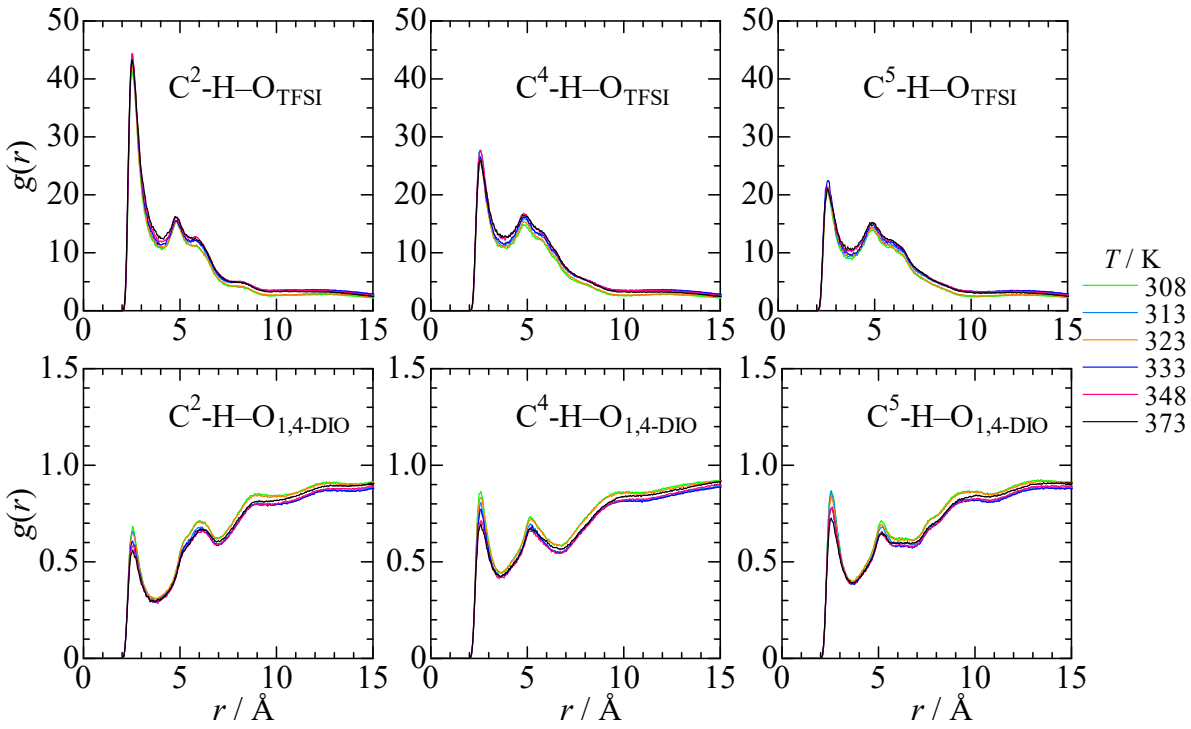

Fig. S22 Temperature dependence of MD pair correlation functions, $g(r)$s, for the $C^{2,4,5}$-H–O_{TFSI} (upper) and $C^{2,4,5}$-H–$O_{1,4\text{-DIO}}$ (bottom) interactions in [C_8mim][TFSI]–1,4-DIO system at $x_{1,4\text{-DIO}}$ = 0.983. The $g(r)$s of the $C^{2,4,5}$-H–O_{TFSI} interactions were calculated for one of the four O atoms within $[TFSI]^-$. The $g(r)$s of the $C^{2,4,5}$-H–$O_{1,4\text{-DIO}}$ interaction were also calculated for one of the two O atoms within 1,4-DIO molecule.

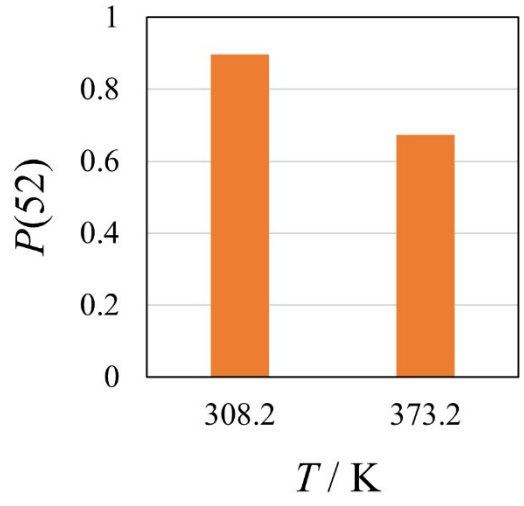

Fig. S23 Temperature dependence of possibility of 52 ions of aggregates, $P(52)$, for 100 ns in [C_8mim][TFSI]–1,4-DIO solution at $x_{1,4\text{-DIO}}$ = 0.983.